

Study of IGZO thin film transistors with Al₂O₃ gate insulator

Shih-Chang Shei* and Yichu Wang

Department of Electrical Engineering, National University of Tainan, Taiwan

Abstract

In this study focuses on the dielectric layer materials of thin film transistors (TFTs). Gate oxide was deposited using a RF Magnetron Sputtering control system. The first studied the aluminium oxide (Al₂O₃) dielectric layer material deposited with different oxygen flow and annealed by the furnace tube. The study found that the properties of aluminium oxide (Al₂O₃) thin film transistors (TFTs) after furnace tube annealing reduced the interface trap density and the roughness of the thin film after annealing. The above dielectric layer is used to make thin film transistors (TFTs) with a bottom gate structure. The characteristics of thin film transistors (TFTs) are significantly improved by higher oxygen flow and additional thermal anneal. By analyzing the structure and electrical measurement of the thin film, the influence of the dielectric layer material on the thin film transistors (TFTs) is analyzed.

Keywords: Indium Gallium Zinc Oxide (IGZO), Thin Film Transistor (TFT), Al₂O₃

* Corresponding author: scshei@mail.nutn.edu.tw
DOI : 10.53106/222344892023041301001

I. INTRODUCTION

AMORPHOUS Indium-Gallium-Zinc-Oxide (a-IGZO) is a promising candidate for high performance TFT because it shows high field-effect mobility and on-current while has very low leakage current, and also, can secure uniform TFT characteristics when fabricated in large area.

Compared to silicon-based TFTs, a-IGZO TFTs have higher transparency over the entire visible range because they have wide band gaps. They also possess better uniformity than polysilicon TFTs because of their amorphous structure [1]. Because amorphous oxides have a more uniform structure and a smoother surface, this can result in a smooth channel interface with the gate insulator [2]. However, the problem of bias stability of a-IGZO TFTs gate bias stress still needs to be solved. According to many studies on the stability of a-IGZO TFTs, bias stability is very sensitive to oxygen vacancies in the a-IGZO film and to ambient oxygen molecules. For these reasons, passivation of oxygen vacancy defects and a-IGZO back channel layers are necessary to maintain good bias stability gate bias stress [1]. The deposition of oxide semiconductors is usually carried out by a simple sputtering method, and maintaining amorphous structure over a large substrate region is a major advantage of such materials [3].

	<i>a-Si TFTs</i>	<i>Poly-Si TFTs</i>	<i>Oxide TFTs</i>
$V_{th} (V)$	> 10V	<0.5V	<1V
<i>Mobility (cm² /Vs)</i>	<1	30-100	1-20
<i>S.S. (V/dec)</i>	< 0.5	0.2-0.3	~0.1
I_{on}/I_{off}	> 10 ⁶	10 ⁷	> 10 ⁹
<i>Light stability</i>	Poor	Good	Superior to a-Si
<i>Uniformity</i>	Good	Poor	Good
<i>Process Temp.(°C)</i>	150–350	250–550	RT–400(600)
<i>Cost</i>	Low	High	Low
<i>yield</i>	High	Low	High

Table.1 The characteristics of a-Si, poly-Si and oxide TFTs [4,5,6,7,8].

As can be seen from the above Table.1, the advantages of oxide TFTs are not only high mobility, but also higher current than amorphous silicon (a-Si) TFTs. The oxide semiconductor has a leakage current of $1 \times 10^{-18} A / \mu m$ or less. For the ON/OFF ratio required for display performance, oxide thin-film transistors (TFTs) shows 10⁹ or higher, which is polycrystalline silicon (10⁷) 100 multiple. Although the mobility of In-Ga-Zn-O TFTs is lower than that of low-temperature poly-silicon (LTPS) TFTs, the fabrication cost is low and the uniformity is better than that of low-temperature poly-silicon (LTPS) TFTs, and large-area displays can be easily fabricated [7].

TFTs can change the structure and shape. TFTs of various structures and compositions can be easily modified or connected to other devices. Once the technical and cost challenges are solved, many new products using TFTs can be realized [4]. TFTs can also be made from a variety of semiconductor and dielectric materials, and variations in threshold voltage and mobility are still difficult to control due to material properties [4,10]. Current TFTs applications are mainly used for pixel driving of large-area LCDs. In large-size display production, display panels will require higher resolution and improved image quality, especially higher brightness, higher contrast, and more. Wide viewing angle and faster response time. Organic and oxide TFTs have been investigated as potential replacements for Si substrate TFTs to reduce production costs or improve mobility. In the near future, advances in TFTs technology may still be driven by the LCD industry [4,11].

II. EXPERIMENTAL DETAILS

In this study, the insulate layer and the active layer were both deposited by RF magnetron sputter system. We studied the effect of oxygen partial pressure (0scm, 5scm) on the properties of Al₂O₃ films under a fixed Ar flow rate and sputtering pressure, and studied the effect of annealing on Al₂O₃ films. The structure of Al₂O₃ deposited under different deposition and process conditions was obtained. Analyze the changes of Al₂O₃ thin film structure

and surface morphology, electrical characteristics and interface trap charge between IGZO semiconductors and the influence of TFT electrical characteristics.

200 nm Al_2O_3 was deposited as insulate layer of the thin film transistor by RF magnetron sputter system, at room temperature with the argon (Ar) gas and the oxygen (O_2) gas were fed into the chamber, the working pressure of 10m Torr, the sputtering power of 200 W, and pre-sputtering is conducted for 10 min to remove impurities and to stability. After the sputtering, the film was annealed at 300°C for 1 hour in atmosphere by anneal furnace. The fabrication conditions are shown in Table.2 and Table.3. The metal mask was fixed on a substrate, 50 nm IGZO was deposited as channel layer of the thin film transistor by RF magnetron sputter system, at room temperature with the argon (Ar) gas at the flow rate of 95 sccm and the oxygen (O_2) gas at the flow rate of 5 sccm were fed into the chamber, the chamber pressured of 10m Torr, the sputtering power of 70 W. After deposition of channel layer, the metal mask was fixed on a substrate to deposit 50 nm Al as source & drain of the thin film transistor, the channel length (L) of 3 mm and the channel width (W) of 4 mm by thermal evaporator.

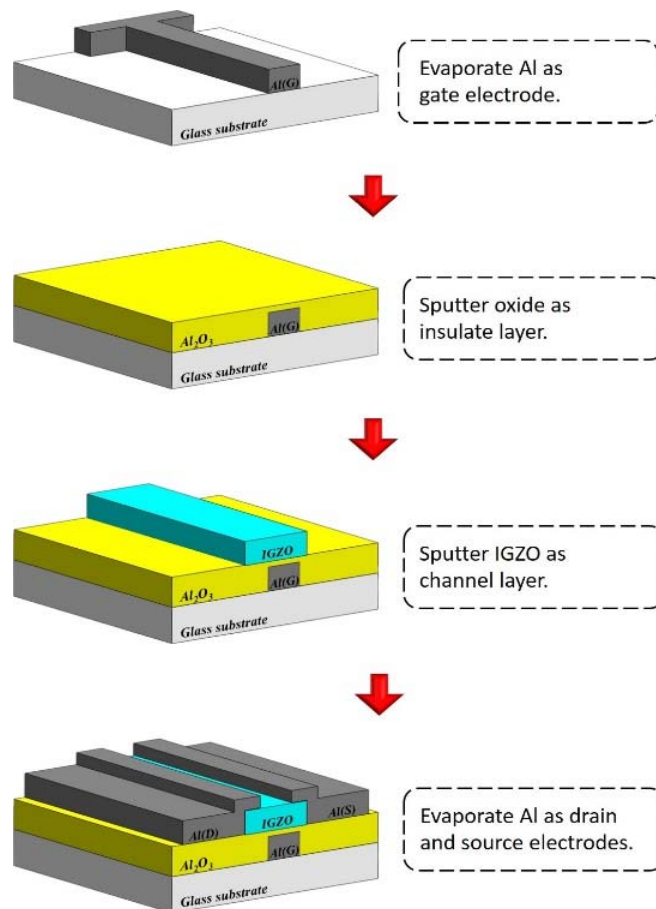


Fig. 1 The flow chart of device fabrication.

	Device A	Device B	Device C
Sputtering gas (Ar : O₂)	30:0 sccm	30:5 sccm	30:5 sccm
Annealing (Temp.)	No annealing	No annealing	Annealing (300°C)

Table. 2 Parameters of the insulate layer for devices.

Parameters	Values
Base pressure (Torr)	8×10^{-6}
Working pressure (mTorr)	10
Sputtering temperature (°C)	Room temperature
Ar : O₂ (sccm)	30:0 (Al ₂ O ₃) 、 30:5 (Al ₂ O ₃) 、 95:5 (IGZO)
RF power (W)	200 W (Al ₂ O ₃) 、 70 W (IGZO)
Deposition rate (nm/min)	3.84 (30:0 sccm) 、 1.89 (30:5 sccm) 、 4.27 (IGZO)
Annealing temperature (°C)	300

Table. 3 Process parameters for the deposition of thin films.

III. RESULTS AND DISCUSSION

A. Surface Analysis

Fig.4 shows an AFM image of the surface morphology of Al₂O₃ films deposited on glass. The root mean square (RMS) roughness of the Al₂O₃ film of device A-C was 2.99, 2.03 and 1.64 nm, respectively. Because of the highest deposition rate in pure Ar, this limits the migration of sputtered atoms, resulting in a maximum surface roughness of the film. The addition of O₂ gas begins to reduce the deposition rate, providing sufficient energy to improve its mobility on the substrate surface, resulting in dense, smooth, and less surface damage. Therefore, the RMS roughness can be reduced by adding oxygen [12,13,14]. The RMS of the deposited film after annealing at 300 ° C will decrease, which means that the film will become denser after annealing.

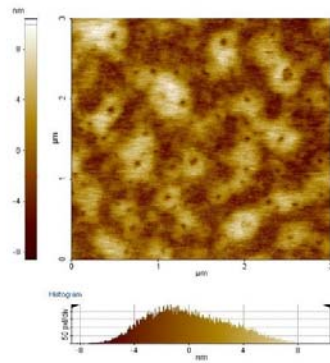


Fig. 2 AFM images of Device A.

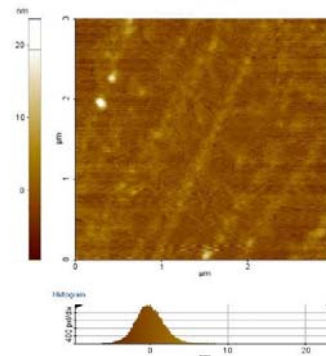


Fig. 3 AFM images of Device B.

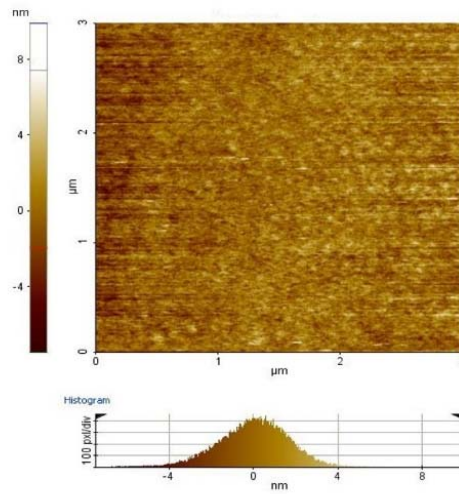


Fig.4 AFM images of Device C.

B. Leakage Current Measurement

The leakage current of the Al_2O_3 dielectric is shown in Fig.5 III. The leakage current of the Al_2O_3 film was 3.82×10^{-4} A, 3.14×10^{-4} A and 2.77×10^{-5} A. Al_2O_3 films are all amorphous films. It is beneficial to suppress leakage current caused by surface roughness. The leakage current in the film deposited under pure Ar and the O_2 flow rate of 5 sccm was almost the same. Annealing at 300°C improves the leakage current of the film. Because the Al_2O_3 film is subjected to an annealing process. Thermal annealing is an effective method to reduce this vacancy [15]. The annealed film improves the passivation of the interface state at the interface, delays the formation of charged defects at the interface, the decrease in leakage current indicates a reduction in defects in the film [16,17,18,19].

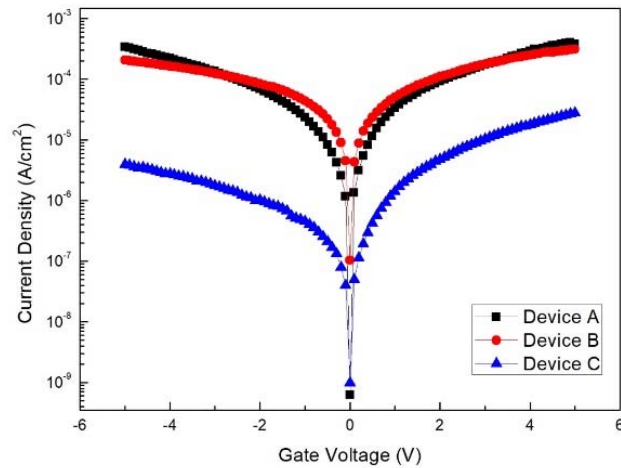


Fig.5 III The leakage current characteristics.

C. Electrical Characteristics of Devices

Fig. 6 shows the capacitance densities of the three gate dielectrics measured at a frequency of 100 kHz. They are 2.35 · 2.64 · 2.84 (nF/cm²). As the flow of O₂ increases, the capacitance shows an increasing trend. After annealing, the device C shows the highest capacitance. The reduction in device A capacitance may be attributed to the porosity of the film deposition, which showed improvement after the film was annealed. This is due to the increase in film density [18].

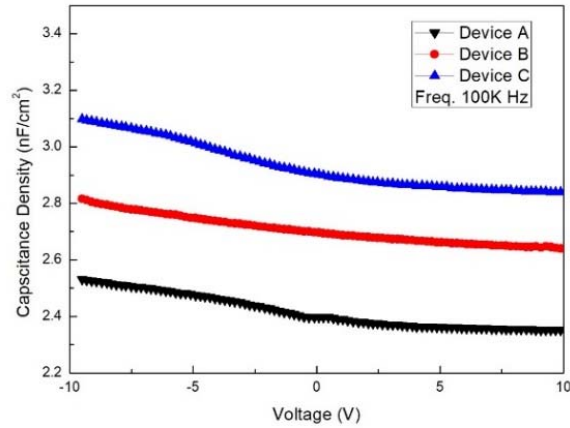


Fig. 6 Capacitance of devices.

D. Leakage Current Measurement

Fig.7 ~ Fig.9 shows the output characteristics of the TFTs with Al₂O₃ insulator different production methods, respectively, Showing a clear pinch-off behavior, all operating in the n-channel enhancement mode [15,20]. When the applied gate voltage (V_{GS}) = 8 V and the source-to-drain voltage (V_{DS}) = 10 V. The maximum saturation currents are 2.82×10⁻⁶ A, 1.61×10⁻⁵ A, and 2.61×10⁻⁵ A, respectively. Device C has the maximum saturation current because a smooth dielectric surface facilitates obtaining a smaller IGZO film trap density and a better dielectric /channel interface. The interface quality can be improved by reducing the interface trap density, to increase the saturation current of the device [21].

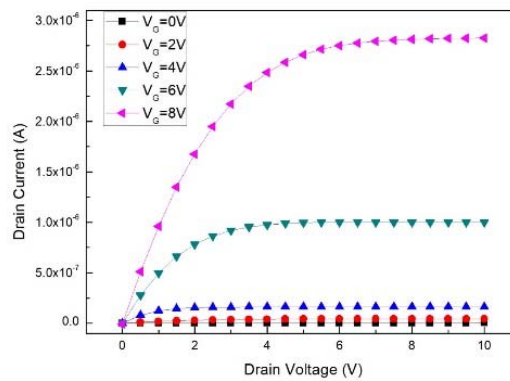


Fig. 7 Output characteristics of device A.

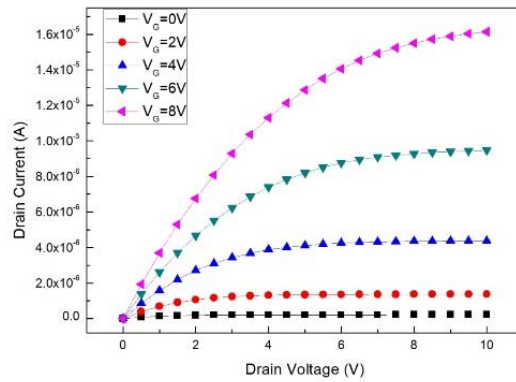


Fig.8 Output characteristics of device B.

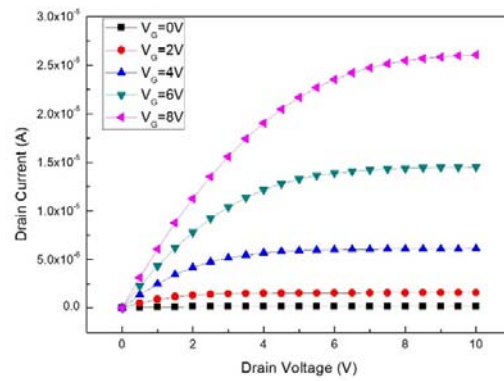


Fig.9 Output characteristics of device C.

To investigate the electrical performance of the device, Fig.10 ~ Fig.12 shows the transmission characteristics of all devices at a fixed drain voltage (V_{DS}) = 10 V. The V_{th} of devices A, B, and C are 6.95, 6.14, and 4.18V, respectively. The calculated mobility of 0.81, 1.06, and 1.56 cm^2/Vs , respectively. The I_{on}/I_{off} ratio of the device is approximately 8.23×10^4 , 4.16×10^5 , and 2.13×10^5 , respectively. The S.S. values of the device were calculated to be 0.21, 0.17, and 0.11 V/decade, respectively. The calculated values of the trap density were 3.7×10^{10} , 3.05×10^{10} , and $1.5 \times 10^{10} \text{ cm}^{-2}$, respectively. Table.4 shows the V_{th} , mobility, I_{on}/I_{off} ratio, S.S, and trap density for different devices.

	$V_{th}(\text{V})$	mobility (cm^2/Vs)	S.S.(V /dec)	I_{on}/I_{off}	$N_t(\text{cm}^{-2})$
Device A	6.95	0.81	0.21	8.23×10^4	3.7×10^{10}
Device B	6.14	1.06	0.17	4.16×10^5	3.05×10^{10}
Device C	4.18	1.56	0.11	2.13×10^5	1.5×10^{10}

Table. 4 The electrical performance of the devices.

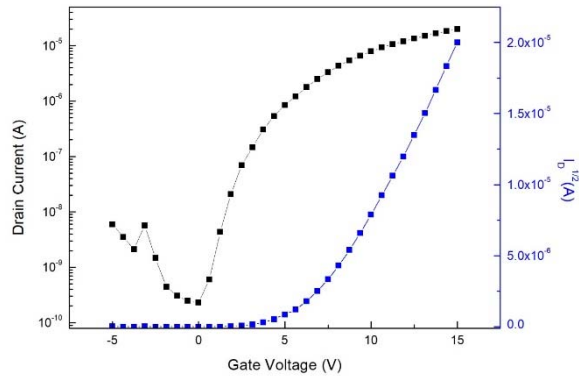


Fig.10 Transfer characteristics of device A.

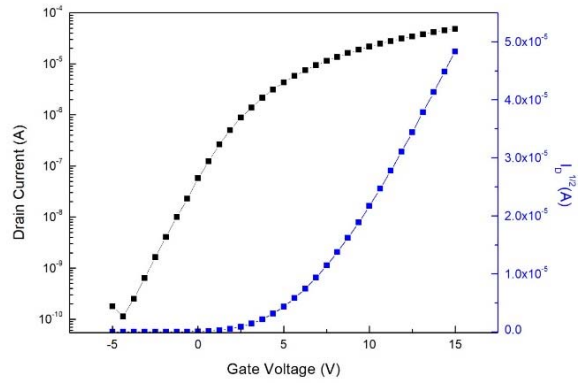


Fig.11 Transfer characteristics of device B.

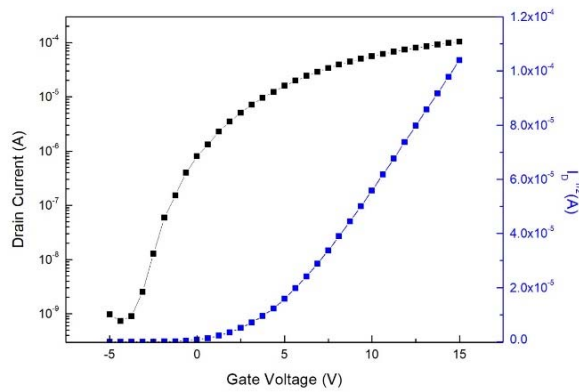


Fig.12 Transfer characteristics of device C.

Dielectric layer roughness is the main factor determining mobility [22]. Increasing roughness reduces mobility, smooth dielectric surfaces cause fewer interface defects, and a better channel- dielectric interface is obtained. Due to fewer interface defects and scattering centers, channel electrons are effectively suppressed, and electrons can be easily

transferred from the source electrode to the drain electrode in the channel. The smooth surface of the dielectric is also conducive to the growth of high-quality IGZO films [23,16,12,24]. Device A has more defects in the channel / dielectric interface and will capture more electrons during operation. Therefore, a larger V_{th} is required to turn on the device [16]. Device C achieved the smallest V_{th} . Because the defects including negative oxide charges generated during the sputtering process can be removed by annealing, the initial positive V_{th} shift caused by the negative oxide charges pre-existing in the dielectric can be reduced [25]. The highest C_{ox} (2.84 nF/cm²) was found after annealing. The increase of C_{ox} leads to a decrease in V_{th} after annealing [26]. S.S. depends on the trap density at the interface between the channel and the gate dielectric. The improvement of S.S. indicates a decrease in interface state [27]. In addition, the switching current ratio (I_{on} / I_{off}) of the TFT also increases with annealing, which is attributed to the decrease in V_{th} and the increase in mobility [28].

IV. CONCLUSION

The experimental results show that a TFT using Al₂O₃ as a gate dielectric layer and IGZO as a channel layer was manufactured. There is no change in the film state of Al₂O₃ after annealing (no crystallization). Annealing has a denser effect, resulting in better film quality and lower surface roughness. It plays an important role in the device's mobility, I_{on} / I_{off} ratio, subthreshold swing. After annealing, the TFT of the Al₂O₃ gate dielectric showed the best performance, the saturation current of 2.61×10^{-5} A, the threshold voltage of 4.18 V, mobility of 1.56 cm² / Vs, an I_{on} / I_{off} ratio of 2.13×10^5 , the subthreshold swing of 0.11 V / decade and surface defects density N_t of 1.5×10^{10} . As the surface state density at the channel-dielectric interface decreases, the dielectric interface is improved, smaller hysteresis changes are obtained, and the stability of the TFT is also improved.

V. REFERENCES

- [1] M.-H. Kim, M.-J. Choi, K. Kimura, H. Kobayashi and D.-K. Choi, "Improvement of the positive bias stability of a-IGZO TFTs by the HCN treatment," *Solid-State Electronics*, vol. 126, pp. 87-91, 2016.
- [2] H. Kumomi, K. Nomura, T. Kamiya and H. Hosono, "Amorphous oxide channel TFTs," *Thin Solid Films*, vol. 516, no. 7, pp. 1516-1522, 2008
- [3] D. G. Yang, H. Do Kim, J. H. Kim, S. W. Lee, J. Park, Y. J. Kim and H.-S. Kim, "The effect of sputter growth conditions on the charge transport and stability of In-Ga-Zn-O semiconductors," *Thin Solid Films*, vol. 638, pp. 361-366, 2017.
- [4] Y. Kuo, "Thin Film Transistor Technology--Past, Present, and Future," *Electrochemical Society Interface*, vol. 22, pp. 55-61, 03/01 2013.
- [5] J.-J. Lih, C.-F. Sung, C.-H. Li, T.-H. Hsiao and H.-H. Lee, "57.1: Invited Paper: Comparison of a-Si and Poly-Si for AMOLEDs," *Sid Symposium Digest of Technical Papers*, vol. 35, 05/01 2004.
- [6] T. Kamiya, K. Nomura and H. Hosono, "Present status of amorphous In-Ga-Zn-O thin-film transistors," *Sci Technol Adv Mater*, vol. 11, no. 4, p. 044305, Aug 2010.
- [7] T. Matsuo, S. Mori, A. Ban and A. Imayama, "8.3: Invited Paper: Advantages of IGZO Oxide Semiconductor," vol. 45, no. 1, pp. 83-86, 2014.
- [8] M. Matsumura, M. Hatano, T. Kaitoh and M. Ohkura, "Subthreshold properties of TFTs with laser-crystallized laterally grown polysilicon layers," *IEEE Electron Device Letters*, vol. 27, no. 4, pp. 278-280, 2006.
- [9] T. Matsuo, S. Mori, A. Ban and A. Imayama, "8.3: Invited Paper: Advantages of IGZO Oxide Semiconductor," vol. 45, no. 1, pp. 83-86, 2014.
- [10] J.-C. Lee, M. P. Hong and J. Y. Jeong, *Low Power Current Mode Poly-Silicon TFT Digital Circuit Design Method for High Speed SOP Components*. 2007, pp. 433-436.
- [11] U. Yasuhiro, "TFT-LCD manufacturing technology — current status and future prospect —," in *2007 International Workshop on Physics of Semiconductor Devices*, 2007, pp. 29-34.
- [12] Y. J. Jo, I.-H. Lee and J. S. Kwak, "In-Ga-Zn-O thin film transistor with HfO₂ gate insulator prepared using various O₂/(Ar+O₂) gas ratios," *Materials Research Bulletin*, vol. 47, no. 10, pp. 2919-2922, 2012.

- [13] X. F. Chen, G. He, M. Liu, J. W. Zhang, B. Deng, P. H. Wang, M. Zhang, J. G. Lv and Z. Q. Sun, "Modulation of optical and electrical properties of sputtering-derived amorphous InGaZnO thin films by oxygen partial pressure," *Journal of Alloys and Compounds*, vol. 615, pp. 636-642, 2014.
- [14] E. Muchuweni, T. S. Sathiaraj and H. Nyakoty, "Effect of O₂/Ar flow ratio on Ga and Al co-doped ZnO thin films by rf sputtering for optoelectronic device fabrication," *Materials Research Bulletin*, vol. 95, pp. 123-128, 2017.
- [15] P. Ma, L. Du, Y. Wang, R. Jiang, Q. Xin, Y. Li and A. Song, "Low voltage operation of IGZO thin film transistors enabled by ultrathin Al₂O₃ gate dielectric," *Applied Physics Letters*, vol. 112, no. 2, 2018.
- [16] Y. Xu, X. Li, L. Zhu and J. Zhang, "Defect modification in ZnInSnO transistor with solution-processed Al₂O₃ dielectric by annealing," *Materials Science in Semiconductor Processing*, vol. 46, pp. 23-28, 2016. [11] U. Yasuhiro, "TFT-LCD manufacturing technology — current status and future prospect —," in 2007 International Workshop on Physics of Semiconductor Devices, 2007, pp. 29-34.
- [17] K. Prabakar, A. Park, N. Cho, W. I. Lee, C. K. Hwangbo, J. G. Lee and C. Lee, "rf-Magnetron sputter deposited ZrO₂ dielectrics for metal-insulator-semiconductor capacitors," *Vacuum*, vol. 82, no. 12, pp. 1367-1370, 2008.
- [18] K. L. Ganapathi, N. Bhat and S. Mohan, "Influence of O₂ flow rate on HfO₂ gate dielectrics for back-gated graphene transistors," *Semiconductor Science and Technology*, vol. 29, no. 5, 2014.
- [19] P. Singh, R. K. Jha, R. K. Singh and B. R. Singh, "Preparation and characterization of Al₂O₃ film deposited by RF sputtering and plasma enhanced atomic layer deposition," *Journal of Vacuum Science & Technology B Nanotechnology and Microelectronics Materials Processing Measurement and Phenomena*, vol. 36, no. 4, 2018.
- [20] J.-M. Lee, B.-H. Choi, M.-J. Ji, J.-H. Park, J.-H. Kwon and B.-K. Ju, "The improved performance of a transparent ZnO thin-film transistor with AlN/Al₂O₃ double gate dielectrics," *Semiconductor Science and Technology*, vol. 24, no. 5, 2009.
- [21] J. Li, F. Zhou, H.-P. Lin, W.-Q. Zhu, J.-H. Zhang, X.-Y. Jiang and Z.-L. Zhang, "SiO_x interlayer to enhance the performance of InGaZnO-TFT with AlO_x gate insulator," *Current Applied Physics*, vol. 12, no. 5, pp. 1288-1291, 2012.
- [22] S. E. Fritz, T. W. Kelley and C. D. Frisbie, "Effect of Dielectric Roughness on Performance of Pentacene TFTs and Restoration of Performance with a Polymeric Smoothing Layer," *The Journal of Physical Chemistry B*, vol. 109, no. 21, pp. 10574-10577, 2005/06/01 2005.
- [23] X. Ding, J. Zhang, W. Shi, H. Ding, H. Zhang, J. Li, X. Jiang, Z. Zhang and C. Fu, "Effect of gate insulator thickness on device performance of InGaZnO thin-film transistors," *Materials Science in Semiconductor Processing*, vol. 29, pp. 326-330, 2015.
- [24] C. Fan, A. Liu, Y. Meng, Z. Guo, G. Liu and F. Shan, "Solution-Processed SrO_x-Gated Oxide Thin-Film Transistors and Inverters," *IEEE Transactions on Electron Devices*, vol. 64, no. 10, pp. 4137-4143, 2017.
- [25] L. X. Qian and P. T. Lai, "Improved Performance of InGaZnO Thin-Film Transistor With HfLaO Gate Dielectric Annealed in Oxygen," *IEEE Transactions on Device and Materials Reliability*, vol. 14, no. 1, pp. 177-181, 2014.
- [26] L. X. Qian and P. T. Lai, "A study on the electrical characteristics of InGaZnO thin-film transistor with HfLaO gate dielectric annealed in different gases," *Microelectronics Reliability*, vol. 54, no. 11, pp. 2396-2400, 2014.
- [27] J. Li, J.-H. Zhang, X.-W. Ding, W.-Q. Zhu, X.-Y. Jiang and Z.-L. Zhang, "Feasibility of using sputtered AlO_x film as gate insulator for high performance InGaZnO-TFTs," *Superlattices and Microstructures*, vol. 65, pp. 14-21, 2014.
- [28] L. X. Qian and P. T. Lai, "Improved Performance of InGaZnO Thin-Film Transistor With HfLaO Gate Dielectric Annealed in Oxygen," *IEEE Transactions on Device and Materials Reliability*, vol. 14, no. 1, pp. 177-181, 2014.